Identification of the Bulk Behavior in the Near-Contact-Surface of Steel Workpieces

A. Dubois, L. Dubar, P. Picart, and J. Oudin

Originally dedicated to the characterization of the material surface properties for processes involving extended workpieces such as tube drawing, the upsetting-sliding test involves a circular cross-section indenter which creates a localized plastic strain by sliding with a given penetration along a generator line of a specimen. The mechanical characteristics of the indenter are the same as those of the tool in the full-scale problem, and the specimen is directly extracted from the workpiece or from the target part of the production plant. An analysis of the upsetting phase of the test is proposed to identify the specimen bulk properties in the near-surface. The stress-strain curve of the specimen is averaged by a Ludwik's model. A dichotomizing search is involved to compute the most suitable Ludwik's parameters by minimizing the error made between experimental results and elastoplastic finite element computations. Identifications carried out on a 1522 annealed steel specimen accurately determined the bulk behavior.

Keywords

bulk behavior determination, elastoplastic finite element analysis, Ludwik's model, steel forming processes, surface vicinity, upsetting-sliding test

1. Introduction

IMPROVEMENTS OF material processing or nonlinear mechanical design problems are strongly related to the bulk and surface material behavior (Ref 1-3).

If a large set of tests is available for the determination of surface behavior (Ref 4), the bulk properties are still currently obtained from tensile or upsetting tests on laboratory specimens. In fact, there may be noticeable differences between the inner bulk properties and the near-surface ones, depending on how the specimen is obtained. The traditional ways of identification become inaccurate when the contact surfaces are important compared to the free ones.

On the other hand, the use of coatings may also affect the specimen bulk behavior, particularly in the case of reacting treatments. The current tendency is to consider coating layers only for their surface effects and ignore their influences on the bulk material characteristics. However, a recent work shows that these coatings do influence the deformed geometry, the stress and strain states of the workpiece in the vicinity of the contact zone (Ref 5). Then, it becomes crucial to develop a new procedure able to quantify these effects and determine the bulk behavior of rolled, laminated, or drawn workpieces, as well as the influence of coatings and surface treatments on the strain hardening of materials.

In the strategy proposed by Bricout et al. to improve surface treatments (Ref 6), the upsetting-sliding test is used to identify surface characteristics at the tool-specimen interface (Ref 7). In the test, a streamlined indenter moves toward the specimen, perpendicularly to its surface, until a required penetration is reached, and then slides along one of its generator lines, creating a local plastic deformation. The mechanical properties of the indenter are the same as the ones of the tool or contactor of the studied process, and the specimen is directly taken in the workpiece of the production plant. The applied loads are measured during indenter displacements; friction stress

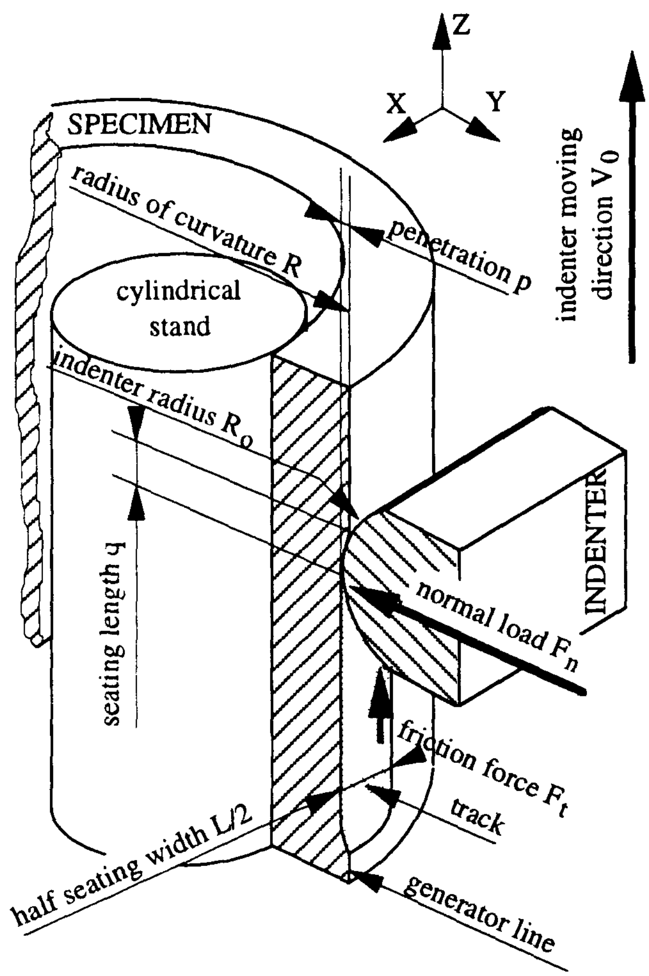

Fig. 1 Main notations and characteristics of the upsetting-sliding test device

J. Oudin, Industrial and Human Automatic Control and Mechanical Engineering Laboratory, CNRS Research Unit 1775, Mecamat, CSMA, University of Valenciennes and Hainaut-Cambrésis, BP 311, F-59304 Valenciennes Cédex, France.

and contact pressure are deduced from mechanical and finite element analyses and lead to an accurate determination of the surface behavior (Ref 8).

In order to complete this surface behavior determination, an analysis of the upsetting phase of the test is proposed to identify the bulk characteristics of the specimen in the neighborhood of the surface. The presented strategy relies on minimizing the error made between experimental measurements and three-dimensional elastoplastic finite element computations of the test. The bulk behavior law of the specimen is averaged by a Ludwik's model. An iterative scheme based on a dichotomizing search is involved. The Ludwik's parameters are used as minimization variables.

2. The Upsetting-Sliding Test

Initially proposed for the analysis of forming processes of extended workpieces, including extrusion, wire, and tube drawing, the upsetting-sliding test reproduces contact conditions that are representative of the studied problem. The indenter penetration and indenter radius are calculated in order to reproduce contact pressure and effective plastic strain at the indenter-specimen interface in the same range as the ones of the full-scale problem. Experiments are operated on specimens which are parts of the real workpieces, ensuring perfect agreement between the mechanical and chemical properties of both the specimen and workpiece.

The upsetting-sliding test device is composed of three main parts: a motionless frame on which the specimen is clamped, a moving frame whose direction of motion is parallel to the generator line of the specimen, and the indenter support lying on the moving frame. The direction of motion of the indenter is perpendicular to the moving frame direction (Fig. 1).

The test operates in two steps. Located 7.5 mm from the bottom of the specimen, the indenter moves normally toward the specimen until the required penetration, then is fastened on the motion frame, which starts its translatory motion (Fig. 2). The indenter displacements in the Z-direction are recorded throughout the experiment. The upsetting-sliding test device is fitted on a standard tensile machine so that the friction force is directly measured by the load cell of the tensile machine. The normal load is derived from the measurement of a special compact strain gage sensor stuck on the indenter support. The penetration is then obtained a posteriori by the measurement of the track left on the specimen. The upsetting phase of the test is used to identify the bulk behavior of the specimen in the neighborhood of the contact zone, and the sliding phase leads to the identification of the surface behavior.

The methodology proposed to identify bulk material behavior at the vicinity of the contact zone is based on minimizing the error between experimental and numerical results. Finite element analyses of the test are achieved, and the mean contact pressure calculated from the contact pressure computed at the indenter-specimen interface is compared to the mean contact pressure derived from experimental measurements.

The indenter penetration is limited to small values during an experiment. We generally take penetration values lower than 0.2 mm to avoid the extension of the plastic zone through the whole thickness of the specimen. Consequently, only the bulk behavior in the near-surface is involved in the identification procedure developed hereafter. Therefore, the bulge created by the displacement of the material under the indenter is insignificant (in fact, no positive node displacements in the Y-direction are observed in the finite element computations). The contact surface is assumed to be equal to the intersection of the cylin-

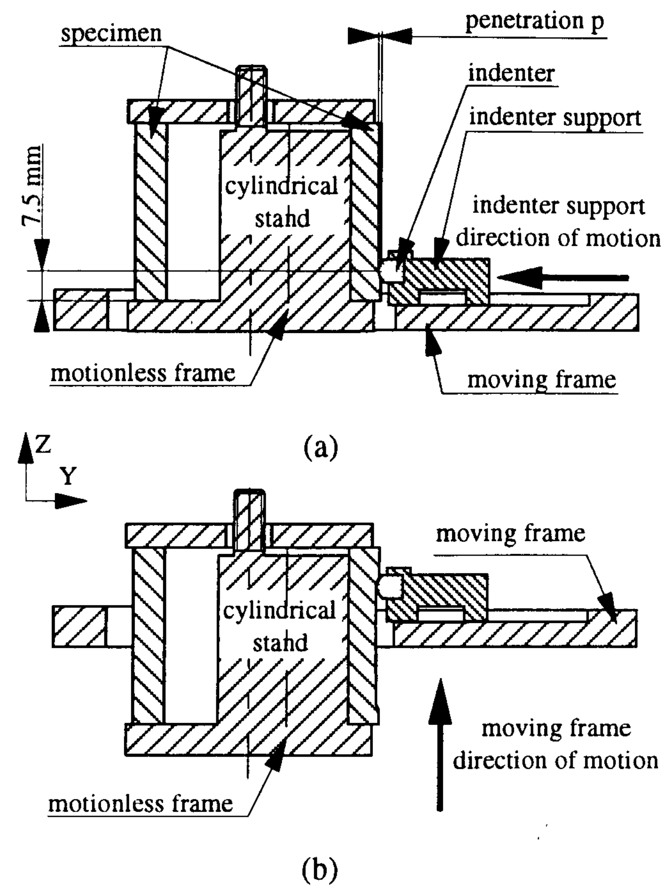

Fig. 2 Cross-sectional view of the upsetting-sliding test device. (a) Upsetting phase. (b) Sliding phase

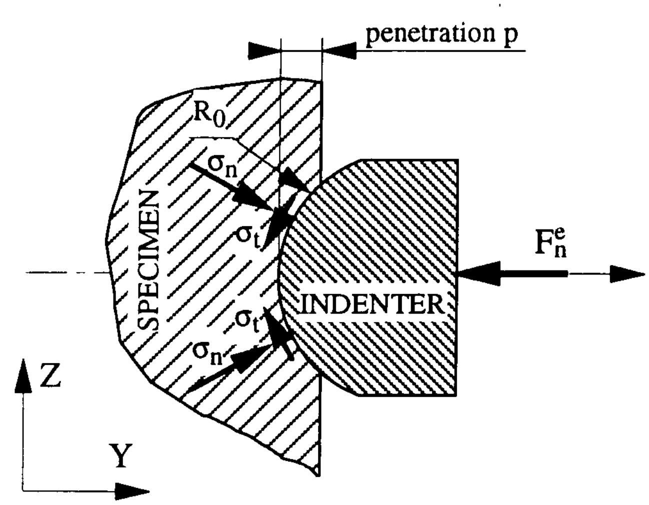

Fig. 3 YZ section of the contact zone in the upsetting-phase of the upsetting-sliding test

drical surface of the indenter with a cylindrical surface of radius R, R being the local radius of curvature of the specimen in the contact zone (the specimen is not necessarily a cylinder or a tube). The indenter penetration, p, is given by:

$$p = R - \sqrt{R^2 - L^2/4} \qquad \text{(Eq 1)}$$

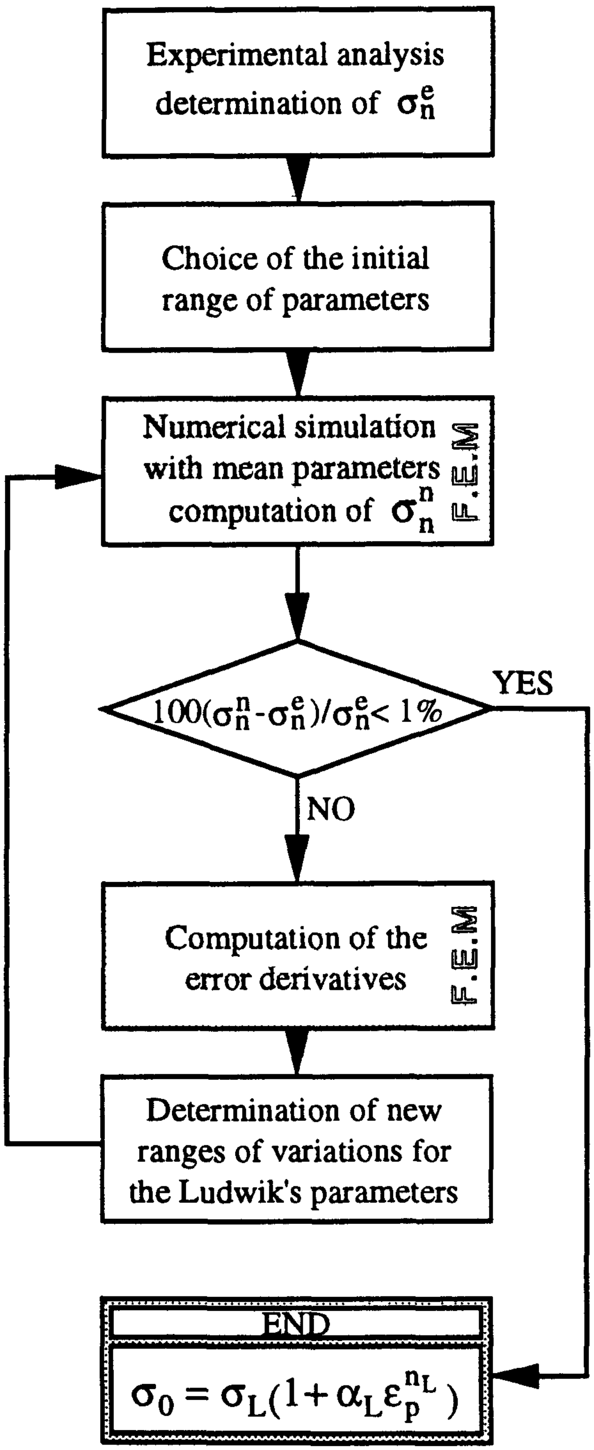

Fig. 4 Identification procedure, global approach. Synopsis of the proposed methodology

where L is the width of the track (Fig. 1). The mean contact pressure exerted at the indenter-specimen interface is then equal to (Fig. 3):

$$\sigma_n^e = F_n^e/\pi L \sqrt{R_0^2 - (R_0 - p)^2} \qquad \text{(Eq 2)}$$

where σ_n^e is the mean contact pressure derived from experimental measurements, F_n^e is the experimental normal load, and R_0 is the indenter radius. Owing to the symmetry of the problem the friction force on the indenter, F_t^e, is equal to zero, and the mean friction stress, σ_t^e, is not to be considered in the analysis.

3. Global Approach to the Identification

3.1 The Identification Procedure

In the proposed strategy to determine the bulk behavior of the specimen, the strain-stress curve is represented by a Ludwik's model:

$$\sigma_0 = \sigma_L(1 + \alpha_L(\varepsilon_p - \varepsilon_i)^{n_L}) \text{ MPa} \qquad \text{(Eq 3)}$$

where σ_0 is the bulk yield stress, ε_p is the effective plastic strain, σ_L, α_L, and n_L are the Ludwik's parameters, and ε_i defines the lower effective plastic strain value from which the bulk yield stress-effective plastic strain relationship is valid. The advantages of this model are the use of the limit of elasticity as a parameter (the σ_L term) and the use of a power function to model the strain hardening; this results in an accurate approximation of the strain-stress curves for plastic strain lower than 0.2 (Ref 9). The Ludwik's model shows very good results in the evaluation of strain-stress relationship of aluminum, titanium, and tungsten alloys (Ref 9-11).

Obviously, the proposed methodology is not linked to the choice of the Ludwik's model; any other parametrized relationship is allowable. Each Ludwik's parameter belong to a given intervals whose boundaries depend on the specimen material. For steel workpieces at room temperature, the Ludwik's parameters are between 50 and 800 MPa for σ_L, 0 and 8 for α_L, and 0 and 1 for n_L. An iterative scheme, which reduces the range of variation of the Ludwik's parameters, is then used to minimize the error made between the mean contact pressure derived from experimental measurements and the mean numerical contact pressure (Fig. 4). A first finite element analysis is run with the mean values of σ_L, α_L, and n_L:

$$\sigma_L^0 = (\sigma_L^m + \sigma_L^M)/2 \qquad \text{(Eq 4)}$$

$$\alpha_L^0 = (\alpha_L^m + \alpha_L^M)/2 \qquad \text{(Eq 5)}$$

$$n_L^0 = (n_L^m + n_L^M)/2 \qquad \text{(Eq 6)}$$

where the superscript 0 is related to the initial values of the Ludwik's parameters in the iterative scheme and the superscripts m and M are related to the lower and upper bounds of the intervals, respectively. Three other simulations are run to evaluate the error derivatives with respect to the Ludwik's parameters:

$$\frac{\partial E^0}{\partial \sigma_L^0} \approx \frac{\Delta E^0}{\Delta \sigma_L^0} = [\sigma_n^n(\sigma_L^0 + \Delta\sigma_L^0, \alpha_L^0, n_L^0) - \sigma_n^n(\sigma_L^0, \alpha_L^0, n_L^0)]/\Delta\sigma_L^0 \quad \text{(Eq 7)}$$

$$\frac{\partial E^0}{\partial \alpha_L^0} \approx \frac{\Delta E^0}{\Delta \alpha_L^0} = [\sigma_n^n(\sigma_L^0, \alpha_L^0 + \Delta\alpha_L^0, n_L^0) - \sigma_n^n(\sigma_L^0, \alpha_L^0, n_L^0)]/\Delta\alpha_L^0 \quad \text{(Eq 8)}$$

$$\frac{\partial E^0}{\partial n_L^0} \approx \frac{\Delta E^0}{\Delta n_L^0} = [\sigma_n^n(\sigma_L^0, \alpha_L^0, n_L^0 + \Delta n_L^0) - \sigma_n^n(\sigma_L^0, \alpha_L^0, n_L^0)]/\Delta n_L^0 \quad \text{(Eq 9)}$$

where σ_n^n is the mean numerical contact pressure and E^0 is the error at the first step of the analysis between experimental and numerical mean contact pressures:

$$E^0 = 100(\sigma_n^n - \sigma_n^e)/\sigma_n^e \quad \text{(Eq 10)}$$

The intervals are then bipartite in regard to the sign of the error E^0 and its derivatives (Fig. 5). As the size of the total problem is divided by eight at each step (2^k where k is the number of parameters), it is considered that the solution will be obtained in a maximum of seven steps, the range of the intervals in progress being then lower than 1% of their original value. The number of computations is also strongly reduced in regard to a classical dichotomizing search, which requires a numerical simulation of the test for each parameter at each bound of the studied domain. Four computations are run with the present method for a three-parameter model, against 27 for a classical dichotomizing search.

3.2 Testing of the Proposed Procedure

The upsetting-sliding experiments analyzed hereafter are achieved on specimens extracted from 1522 annealed steel tube of outer diameter 70 mm and inner diameter 58 mm. In order to determine the bulk material behavior of this material and have a reference to validate the identification procedure, small cylinders are machined from the tube. They are polished and lubricated so that the Coulomb's friction coefficient at the die-cylinders interface is equal to 0.07. Their initial dimensions are shown in Fig. 6(a). The cylinders are submitted to a reduction of height of 50%, which corresponds to an effective plastic strain equal to 0.69. The strain-stress relationship is derived from the force-displacement curves recorded during the tests. It is found that

$$\sigma_0 = 248.94\ (1 + 2.85\varepsilon_p^{0.226})\ \text{MPa} \quad \text{(Eq 11)}$$

The bulk behavior of the 1522 annealed steel being identified, the global approach is applied to these upsetting tests in order to quantify the accuracy of the proposed procedure. The mesh of the cylinders involves 53 axisymmetric elements with four nodes and four integration points and two axisymmetric elements with three nodes and one integration point (Fig. 6b). The total number of degrees of freedom is 140.

Figures 7 and 8 present the evolutions of the error E and its derivatives for two sets of initial ranges of parameters. It appears that the evolutions of the Ludwik's parameters are interdependent; the signs and values of the derivatives remain almost constant whatever the values of the current parameters in progress.

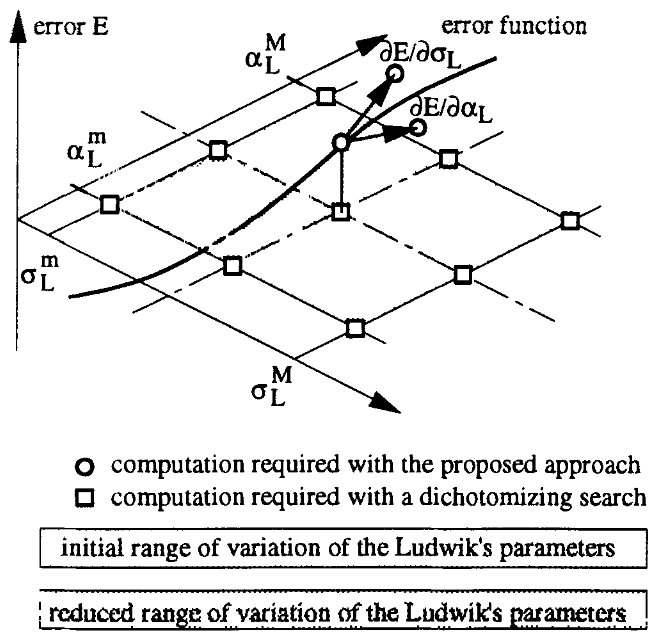

Fig. 5 Identification procedure, global approach. Principle of the reduction of the range of variation of the Ludwik's parameters, presented for a two-parameter model

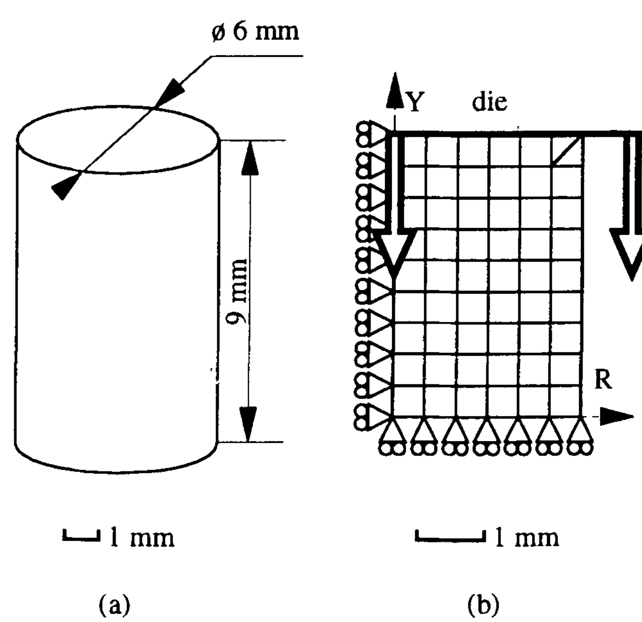

Fig. 6 Identification procedure, global approach. (a) Main dimensions and (b) finite element mesh of the cylinders

One consequence is that the convergence of the procedure toward two different laws depends on the initial range of variations of the Ludwik's parameters (Fig. 9). The experimental curve and the first numerical identified curves are in good agreement, but great differences arise between the experimental curve and the second identified curves. The three curves are in concordance only in the effective plastic strain range going from 0.6 to 0.8. That corresponds to the strain measured within the specimen: the proposed strategy in its current state is only able to identify bulk properties of the specimen in a range of effective plastic strain. This consequence is based on the fact that only the final state of the specimen is considered in the methodology, not the history of the deformation. The solution is to build the bulk yield stress-strain curve from several tests achieved at different strain states using a stepwise procedure. The application of this method to the upsetting phase of the upsetting-sliding test is presented below.

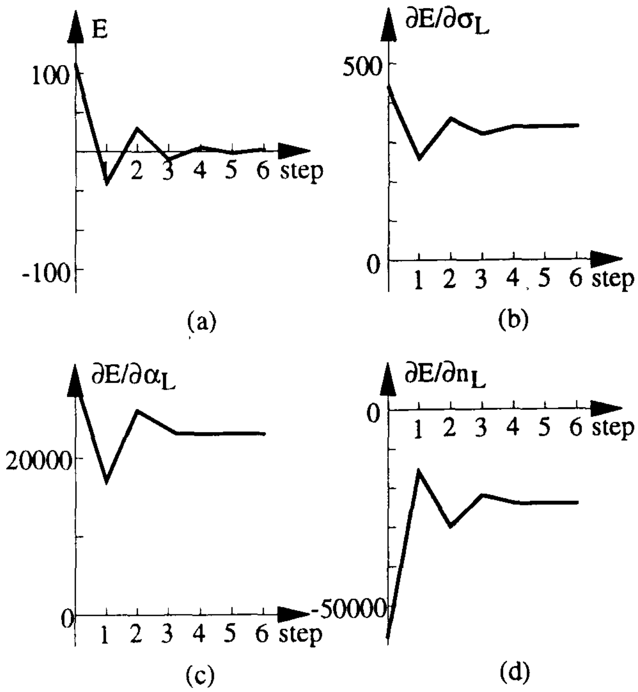

Fig. 7 Identification procedure, global approach. Variation of the error E and its derivatives for initial parameters equal to 400 for σ_L, 4 for α_L, and 0.2 for n_L

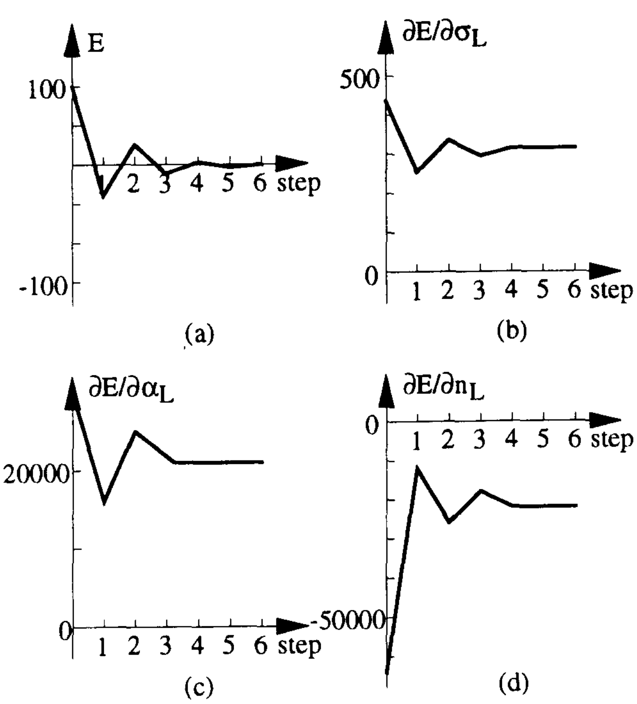

Fig. 8 Identification procedure, global approach. Variation of the error E and its derivatives for initial parameters equal to 400 for σ_L, 4 for α_L, and 0.4 for n_L

4. Stepwise Identification

4.1 Step-by-Step Identification Procedure

Because the evolution of the three Ludwik's parameters is interdependent, the new identification can be achieved with a one-parameter-behavior law. Consequently, only one numerical simulation is required at each step of the procedure to compute the error E, its derivative in regard to the parameter being calculated once at the first iteration. The total number of computations remains approximately the same as the global approach, although there are more tests to analyze.

However, the course of the parametrized bulk yield stress/effective plastic strain curves has to be similar to the course of the one researched to respect the deformation path and consequently to converge toward strain and stress distributions close to the real ones. Therefore, a Ludwik's model that

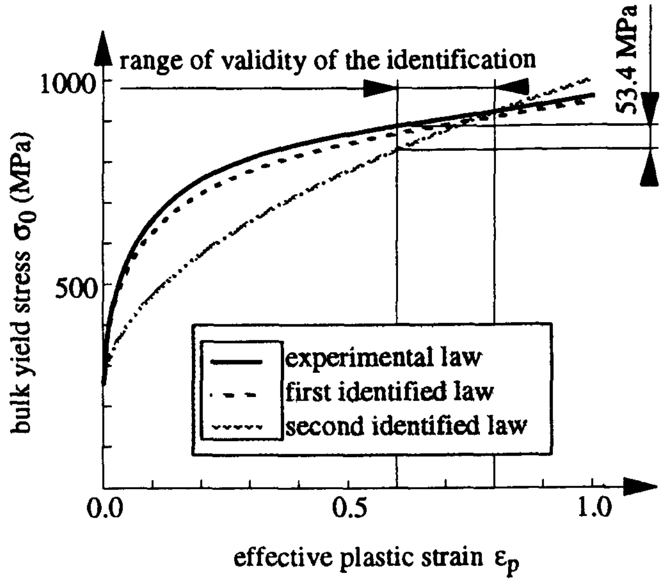

Fig. 9 Identification procedure, global approach. Comparison between the experimental bulk behavior law and the bulk behavior laws resulting from the identification procedure. First identified law: $\sigma_0 = 262.50\ (1 + 2.625\ \varepsilon_p^{0.269})$ MPa. Second identified law: $\sigma_0 = 270.31\ (1 + 2.703\ \varepsilon_p^{0.530})$ MPa

fits well with the course of steel bulk behavior curves is used. Two of its parameters are fixed; only the hardening coefficient varies, from 0 to 1.

The new identification strategy is based on the data processing of a series of tests. The identification is achieved for each test using the iterative scheme presented in the global approach, so that a set of different Ludwik's curves is obtained. The range of validity of the identified curves is given by the range of effective plastic strain computed in the specimen by the finite element code. The bulk behavior law of the analyzed material is interpolated from the couples of maximum effective plastic strain/maximum bulk yield stress (ε_p, σ_0) computed in the corresponding range of validity for each test (Fig. 10). Therefore, the result of the final identification is independent of the choice of the Ludwik's parameters used in the iterative scheme.

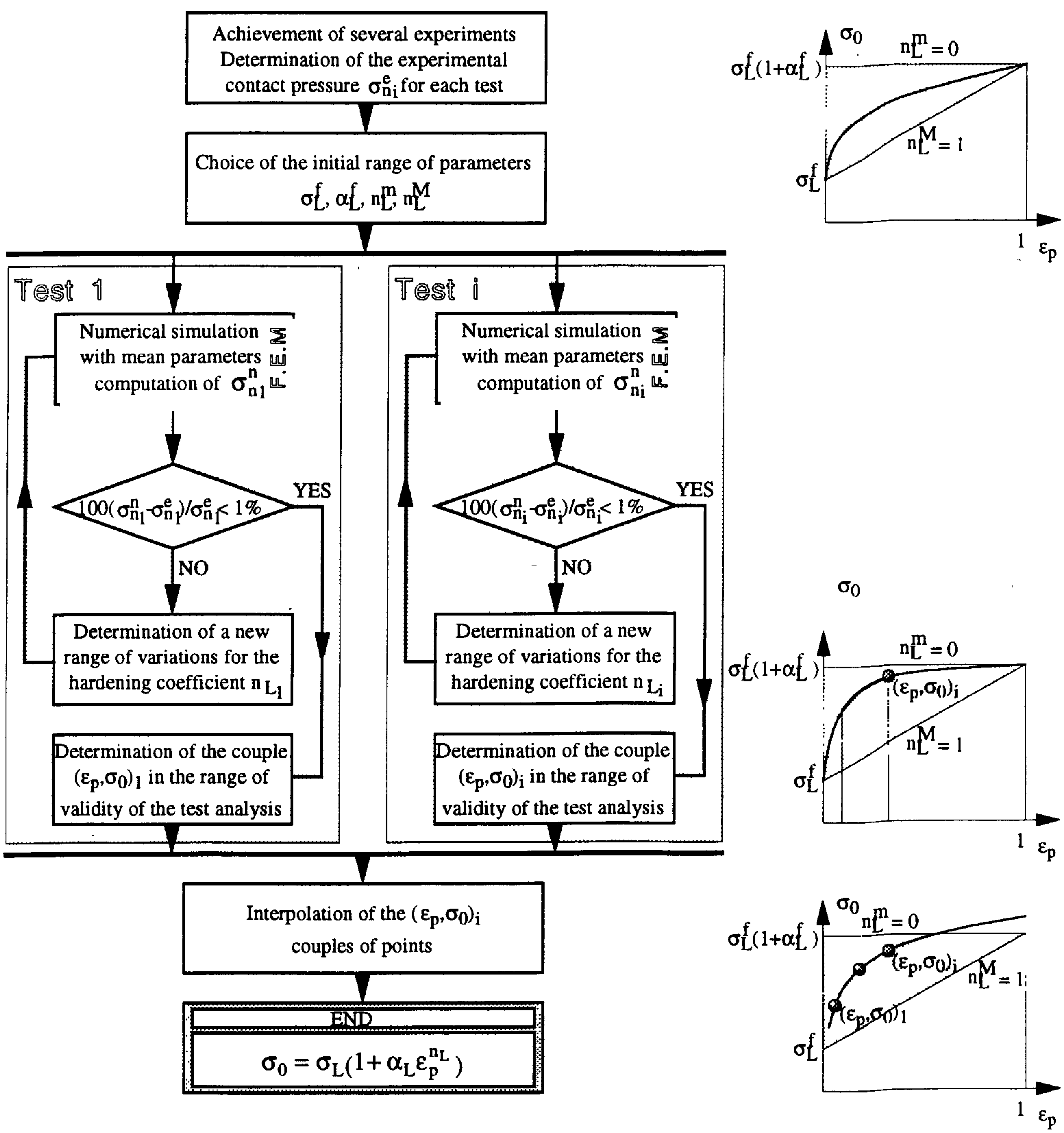

Fig. 10 Identification procedure, step-by-step approach. Synopsis of the proposed methodology

4.2 *Application to the Upsetting Phase of the Upsetting-Sliding Test*

The upsetting-sliding test was originally devoted to the characterization of the surface behavior of processes involving extended workpieces, such as wire drawing, where the encountered effective plastic strain are between 0.05 for skeen pass to 0.2 for wire reduction of 20%. The step-by-step procedure first used to identify the bulk behavior of the specimen in that range of effective plastic strain. On the other hand, that range of effective plastic strain greatly determines the course of the Ludwik's curve for higher values of effective plastic strain ($0.2 \leq \varepsilon_p \leq 1$). It is then expected that a curve accurately identified for effective plastic strain ranging from 0.05 to 0.2 will provide a good approximation of the bulk behavior in a wider range of effective plastic strain, the range of validity of the identification being then extended to an enlarged range of use.

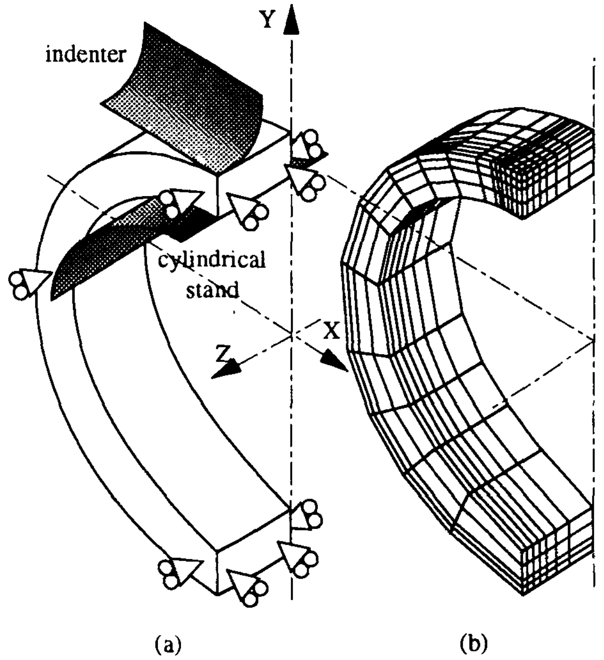

Fig. 11 Identification procedure, step-by-step approach. (a) boundary conditions and (b) finite element mesh of the specimen

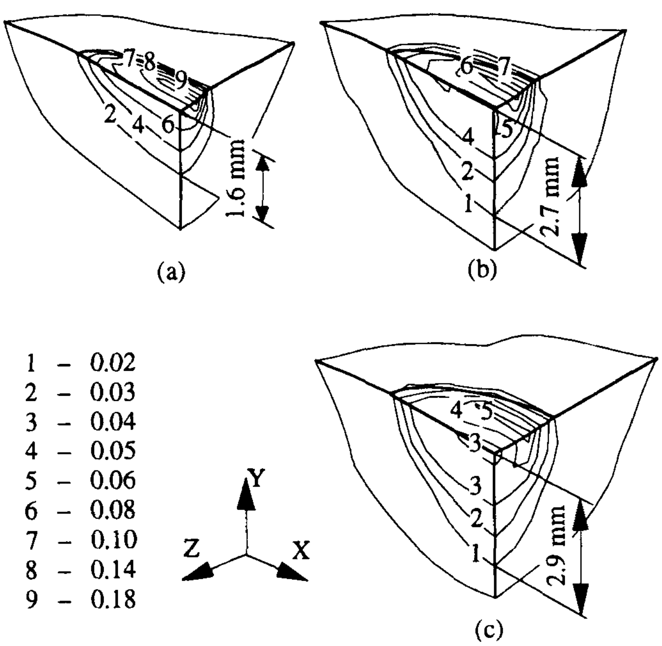

Fig. 12 Identification procedure, step-by-step approach. Effective plastic strain distributions in the vicinity of the contact zone for indenter penetration of 0.16 mm and indenter radii equal to (a) 2 mm, (b) 5 mm, and (c) 10 mm

The identification is based on the local upsetting of 70 mm diameter 1522 annealed steel specimens of 50 mm length with G1 carbide tungsten indenter, the specimen bulk behavior being the same as the ones of the 6 mm diameter specimen already studied.

A first three-dimensional finite element mesh is defined by modeling one-half of the specimen. According to the symmetry conditions, the X-displacements of nodes located in the X = 0 plane fixed to 0. As the specimen is clamped on the device, the Z-displacements of nodes located in the Z = 0 and Z = 50 mm planes also fixed to 0. In order to compute accurate stress and strain distribution at the indenter-specimen interface, seven discretization segments in the X-direction and eight in the Z-direction are involved to model the contact surface. The mesh consists of 17 layers of three-dimensional elastoplastic elements with eight nodes and eight integration points in the circumferential direction, 24 layers in the Z-direction, and four layers through the specimen thickness. The element size are smaller and smaller as the element is closer to the contact zone. A total of 6750 degrees of freedom is then used.

The stiffnesses of the indenter and of the cylindrical stand on which the specimen is leaned are far more significant than that of the specimen, so the indenter and the cylindrical stand are modeled by cylindrical rigid surfaces, the contact being considered unilateral. The contact at the indenter-specimen interface is controlled by 28 interface elements with one node.

Two computations are run, with Coulomb's friction coefficients equal to 0 or 0.3, respectively corresponding to perfect conditions of contact and bad mixed lubrication regime. The bulk behavior used for these analyses is the experimental one given in Eq 11. It can be noticed that:

- The stress and strain distributions are symmetric in regard to the symmetry plane of the indenter (Z = 7.5 mm).
- The stress and strain distributions remain confined between the Z = 2 and Z = 13 mm planes.
- The stress and strain are not significantly influenced by the friction coefficient.

A new model is then involved to model the specimen from Z = 0 to Z = 7.5 mm and involving a zero friction stress. The boundary conditions are similar to those of the previous model, except that symmetry conditions are added for the node located in the Z = 7.5 mm plane. The new model involves 476 elastoplastic elements with eight nodes and eight integration points, 28 contact elements, and 2160 degrees of freedom (Fig. 11).

The effective plastic strain reached at the indenter-specimen interface is strongly related to the indenter radius, R_0, and penetration, p. For finite element computations of the test performed with indenter radii ranging from 2 to 10 mm and an indenter penetration equal to 0.16 mm, the maximum effective plastic strain values increase from 0.06 to 0.18 (Fig. 12). The depth of the plastic zone remains in these cases lower than one-half the thickness of the specimen (3 mm); the identification concerns mainly the bulk behavior at the near-surface of the specimen.

A set of experiments were performed with indenter radii of 2, 5, and 10 mm and an indenter penetration of 0.16 mm. Three identifications were performed with different sets of initial parameter values. The results are shown in Table 1. The range of validity of the identifications is 0.03 to 0.18, which corresponds to the maximal and minimal effective plastic strain computed at the indenter-specimen interface in the three tests. An excellent agreement is observed between the experimental laws obtained from Eq 11 and the identified laws, the error between the curves being lower than 5% for ε_p between 0.03 and 1 (Fig. 13). The range of use of the identified bulk behavior law is then extended.

5. Conclusions

The upsetting-sliding test is devoted to the determination of friction laws and to the identification of friction coefficient and factor. The test involves a streamlined indenter that exerts a given contact pressure on a specimen by sliding along one of its generator lines with a prescribed penetration. The test operates in two steps: the indenter moves toward the specimen until the required penetration is reached, then slides along the specimen

Table 1 Results of the identification procedure

Initial parameters						
Fixed		Variable	Indenter radius (R_0), mm			Identified Ludwik's laws
σ_L	α_L	n_L	10	5	2	(range of validity: $0.03 \le \varepsilon_p \le 0.2$)
250	3.00	$0 \le n_L \le 1$	0.25	0.24	0.23	$529.92\,(1 + 0.907\,(\varepsilon_p - 0.03)^{0.398})$
300	3.00	$0 \le n_L \le 1$	0.38	0.37	0.36	$536.43\,(1 + 0.936\,(\varepsilon_p - 0.03)^{0.443})$
250	2.00	$0 \le n_L \le 1$	0.15	0.12	0.10	$540.48\,(1 + 0.841\,(\varepsilon_p - 0.03)^{0.451})$

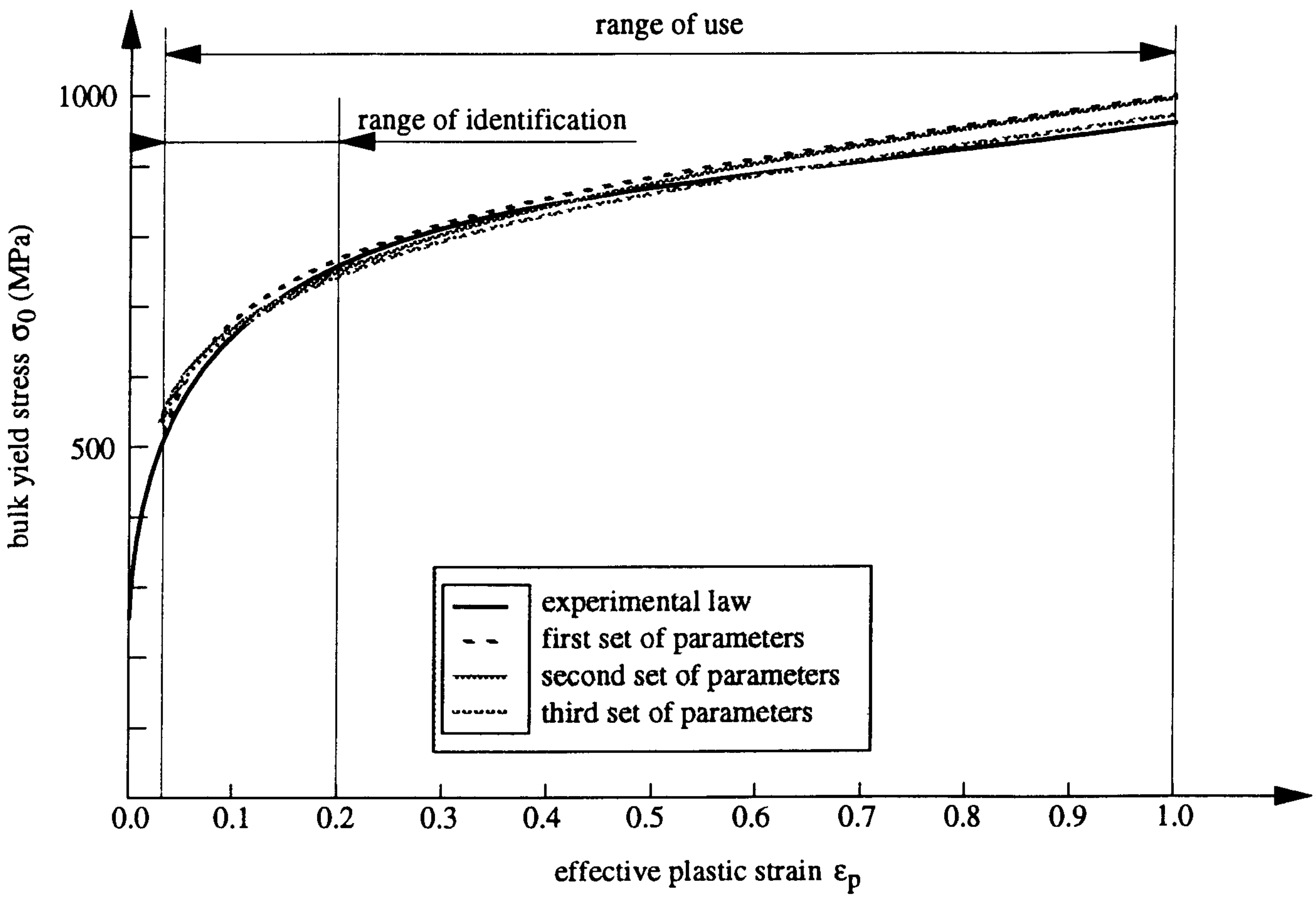

Fig. 13 Identification procedure, step-by-step approach. Comparison between the experimental bulk behavior law and three laws identified with different initial parameter ranges of variations

surface. An analysis of the first phase of test is presented to identify the bulk behavior of the specimen in the neighborhood of the contact surface.

The proposed methodology is based on minimizing the error made between the contact pressures derived from experimental measurements and the contact pressures resulting from finite element computations. It involves several tests leading to different strain states and an iterative scheme derived from a dichotomizing search. The results of the identification of each test are gathered and lead to the identification of a global bulk yield stress/effective plastic strain. It has been shown that:

- The combination of several identifications involving results from different experiments leads to an accurate determination of the bulk properties of the specimen for effective plastic strain in the ranging from 0.03 to 1.
- The results of the identification are independent of the initial values of the identification parameters.
- The procedure presented to identify the bulk properties of materials is not restricted to the upsetting-sliding test; it is applicable to any process since only the confrontation between experimental and numerical results is required.
- In the case of the upsetting-sliding test, the stress and strain distributions remain confined near the contact zone. Therefore, the procedure allows determination of the bulk behavior in the vicinity of the specimen surface.

Due to its ability to identify material behavior in a restricted zone of a workpiece, the proposed identification method is promising for the determination and identification of bulk properties of industrial materials, particularly in the case of coating billets and workpieces with nonhomogeneous characteristics. The determination of accurate bulk behavior in the vicinity of contact surfaces is an important step toward the determination of reliable friction constitutive equations where the friction coefficients and factors are commonly expressed as functions of the bulk and shear yield stresses.

Acknowledgments

The present research work has been supported by CNRS, Conseil Régional Nord—Pas de Calais, Ministère de l'Education Nationale, and Délégation Régionale du Ministère de la Recherche et de la Technologie. The authors gratefully acknowledge these institutions.

References

1. D. François, A. Pineau, and A. Zaoui, *Comportement Mécanique des Matériaux*, Eds Hermes, Paris, 1991
2. J.A. Schey, *Tribology in Metalworking—Friction, Lubrication and Wear,* American Society for Metals, 1983
3. J.T. Oden and J.A.C. Martins, Models and Computational Methods for Dynamic Friction Phenomena, *Comp. Meth. Appl. Mech. Eng.*, Vol 52, 1985, p 527-634
4. J. Oudin, J.M. Rigaut, J.C. Gélin, D. Lochegnies, and J.P. Bricout, Approches Expérimentales et Numériques des Conditions de Contact et de Frottement, *Physique et Mécanique de la Mise en Forme des Métaux,* F. Moussy and P. Franciosi, Ed., Presses du CNRS, Paris, 1990, p 406-435
5. C. Wierre, J.D. Guérin, J. Oudin, and J.P. Bricout, Finite Element Analysis of the Beginning of the Indentation-Rotation Test for Phosphate and Stearate Coatings, *J. Mater. Proc. Technol.,* Vol 41, 1994, p 171-185
6. J.P. Bricout, J. Oudin, J.M. Rigaut, J. Cabezon, and Y. Ravalard, Méthodologie d'Optimisation des Traitements de Surface avant Déformation à Froid par Étirage, *La Revue de la Métallurgie—CIT,* April 1990, p 393-404
7. J.M. Rigaut, J. Oudin, J.P. Bricout, J. Cabezon, and Y. Ravalard, A New Test Procedure for the Improvement of Drawing and Similar Processes, *J. Mater. Proc. Technol.,* Vol 3, 1990, p 3-28
8. P. Picart, J. Oudin, and A. Dubois, On the Determination of Friction in the Cold Forging of Coated Workpieces, *Proc. 9th Int. Cold Forging Congress 1995,* FMJ Int. Pub. Ltd., Redhill, UK, 1995, p 185-191
9. H.W. Rosenberg, Stress-Strain Curves in Alpha Ti Alloys—Some Problems and Results, *Metall. Trans. A,* Vol 8, 1977, p 451-455
10. E. Nes, A.L. Dons, and N. Ryum, Substructure Strengthening of Cold Rolled Aluminium Alloys, *Proc. 6th Int. Conf. of Strength of Metals and Alloys,* Pergamon Press, Vol 1, 1983, p 425-430
11. K.B. Povarova, Yu.O. Tolstobrov, and E.K. Zavarina, Changes in the Structure and Properties of Heterophase Tungsten Alloys, *Metalloved. Term. Obrab. Met.,* No. 6, 1987, p 38-41